Optimizing bidirectional impulse turbines for thermoacoustic engines

Michael A. G. Timmer, and Theo H. van der Meer

ARTICLES YOU MAY BE INTERESTED IN

Characterization of bidirectional impulse turbines for thermoacoustic engines
The Journal of the Acoustical Society of America **146**, 3524 (2019); https://doi.org/10.1121/1.5134450

Review on the conversion of thermoacoustic power into electricity
The Journal of the Acoustical Society of America **143**, 841 (2018); https://doi.org/10.1121/1.5023395

Determination of propagation model matrix in generalized cross-correlation based inverse model for broadband acoustic source localization
The Journal of the Acoustical Society of America **147**, 2098 (2020); https://doi.org/10.1121/10.0000973

A comparison of compressive equivalent source methods for distributed sources
The Journal of the Acoustical Society of America **147**, 2211 (2020); https://doi.org/10.1121/10.0001073

Estimation of seabed properties and range from vector acoustic observations of underwater ship noise
The Journal of the Acoustical Society of America **147**, EL345 (2020); https://doi.org/10.1121/10.0001089

A denoising representation framework for underwater acoustic signal recognition
The Journal of the Acoustical Society of America **147**, EL377 (2020); https://doi.org/10.1121/10.0001130

Optimizing bidirectional impulse turbines for thermoacoustic engines

Michael A. G. Timmer[a)] and Theo H. van der Meer

Department of Thermal Engineering, University of Twente, Enschede, The Netherlands

ABSTRACT:

The design of a bidirectional impulse turbine to convert thermoacoustic power into electricity is experimentally optimized. The turbine efficiency is measured for rotors with and without a shroud ring and for a varying tip clearance. Furthermore, the axial spacing between the guide vanes and rotor is varied with respect to the displacement amplitude of the acoustic wave. All measurements are carried out for several turbine loads and acoustic frequencies. For a chosen implementation, a design study on the guide vane and rotor blade geometry is presented to further optimize the bidirectional impulse turbine for thermoacoustic engines. © 2020 Acoustical Society of America.

https://doi.org/10.1121/10.0001067

I. INTRODUCTION

Thermoacoustic devices convert heat into acoustic power using the thermoacoustic effect. Since devices can be built that work on a temperature gradient as small as 30 K with the surroundings,[1] the focus of thermoacoustic machines is usually on low-grade heat, such as waste heat[2] or solar heat.[3,4] Once acoustic power has been produced, it is generally used to produce cooling through the same thermoacoustic effect. This results in a refrigeration device working purely on heat as an input, besides the small amount of electricity needed to pump the working fluids through heat exchangers. A way to make such a machine work completely without external electricity is to use a fraction of the acoustic power to internally produce the needed electricity.

Acoustic power can be converted into electricity by using a linear alternator, which is a specialized loudspeaker that is driven in reverse. These linear alternators have been shown to be effective in converting the acoustic power, but they are generally expensive and have problems when scaling to industrial sizes.[5] Another widely investigated option is the use of piezoelectric transducers to convert acoustic power into electricity,[6] but so far this has only been demonstrated on a small scale.[5] An alternative that does scale well with increasing size is a bidirectional turbine, which has already been shown in oscillating water columns (OWCs) to convert bidirectional wave energy into electricity with powers reaching up to 1 MW.[7] Previous work has confirmed that a bidirectional impulse turbine can also convert acoustic power into electricity for a range of thermoacoustic conditions.[8] This work has mainly focused on proving the concept and characterizing the performance of a first turbine prototype. The maximum efficiency of the turbine was found to be 25%, which is significantly lower than the 37% efficiency

for the turbine in an OWC on which the first prototype was based.[9]

This work will focus on optimizing the efficiency of the bidirectional impulse turbine by experimentally investigating the influence of design changes for varying thermoacoustic conditions. The optimization is mostly based on work done for OWCs, but it should be kept in mind that the operating conditions in thermoacoustic engines are quite different. For example, the frequency is approximately 3 orders of magnitude higher and the pressure and velocity run partly out of phase. It is therefore interesting to investigate design changes since the turbine efficiency might not be affected in the same manner as for OWCs (or steady flow turbomachinery).

For OWCs, there is no significant influence on the turbine efficiency for varying the axial spacing between the guide vanes and the rotor.[9] However, for thermoacoustic conditions the influence of the axial spacing could be important, since the displacement amplitude of the gas can be so small that it is in the same order of magnitude as the turbine dimensions. Therefore, the influence of the axial spacing will be investigated in Sec. V. Before examining this, the effect of adding a shroud ring around the rotor blades is investigated in Sec. III. This is done in an effort to increase the turbine efficiency by reducing the tip leakage, where the latter is shown to have an especially large effect for relatively big tip clearances.[10] Following this, the tip clearance of both unshrouded and shrouded rotors is varied in Sec. IV. With respect to the first prototype, it is expected that the efficiency can be significantly improved in this manner, since the tip clearance was relatively large for that turbine. Once the optimal axial spacing and tip clearance are set, a design study varying the turbine geometry is presented in Sec. VI. Since the guide vanes and rotor are chosen as the optimum ones found for a design study in OWCs,[9] the main focus of this section is to identify whether this design is also optimal for thermoacoustic conditions.

a)Electronic mail: timmer.mag@gmail.com, ORCID: 0000-0001-6008-8903.

II. EXPERIMENTAL SETUP

This section will provide details about the experimental setup that is used for this work. A more elaborate explanation about the experimental procedure, including processing, validation, and error estimation, can be found in previous work.[8] The raw data, processing scripts, and processed results for all experiments presented in this work can be found in a supplementary data publication.[11]

The experimental setup is shown schematically in Fig. 1. A 15 in. loudspeaker (JBL W15GTi) is connected to the straight tube section through an exponential horn. The loudspeaker is driven by a 2 kW audio amplifier (Behringer EP2000) that is controlled by a computer sound card. For the used frequencies of 50–80 Hz, the pressure amplitude of the sound wave can reach up to 7500 Pa in the turbine section due to the contracting exponential horn and the closed end. The pressure is measured by four piezoresistive pressure sensors (Honeywell 26PCAFA6D) mounted flush with the tube wall. By using two pressure sensors on either side of the turbine, the local acoustic power is calculated by the two-sensor method given by Fusco et al.[12] The input power to the turbine is determined by the difference between the acoustic powers, which is denoted by the acoustic power drop, ΔE_2.

The bidirectional turbine is connected to a brushless electric motor (Hacker A10–13L) that is used as a generator. The three-phase current from the generator is delivered to the electrical load, which consists of a set of precision resistors. Three different sets of resistors, namely, R = 4.7 Ω, 10 Ω, and 20 Ω, are used to vary the turbine RPM for a given acoustic power. By measuring the produced voltage over one resistor, the electrical output power is determined. To convert this to the produced shaft power of the turbine, the generator efficiency has been calibrated for all loads in the range of 1000–8000 RPM. By dividing the electrical power with the generator efficiency, the shaft power is calculated. Subsequently dividing the shaft power with the acoustic power drop yields the efficiency of the bidirectional impulse turbine, η_t. Following the error estimation procedure from previous work[8] and extrapolating for the current turbines, it can be said that results that show more than 0.8% difference in turbine efficiency can be regarded as reliable.

The turbine designs that are used in this work are based on a design from Suzuki et al. for an OWC.[13] A detailed schematic of the turbine design will be presented in Sec. VI along with a design study. The nominal turbine as it is mounted in a tube section is shown schematically in Fig. 2. The nominal turbine consists of a rotor with 29 blades, enclosed by two guide vanes with 26 blades each. The generator is mounted on a guide vane and is concentrically connected to the rotor with a prop adapter. Elliptic nose cones that reach up to the hub radius are connected to both guide vanes to ensure the flow is redirected towards the blades. The rotor, guide vanes, and nose cones are all 3D printed from PA 2200 plastic using selective laser sintering.

To fix the whole turbine assembly in the setup, the guide vanes have shroud rings that tightly fit in the outer tube. The rotor is shown without a shroud ring in Fig. 2, but many rotors in this work do have such a ring and will be referred to as shrouded rotors. The difference between shrouded and unshrouded rotors will be investigated in Sec. III. Either with or without ring, the distance from the tip of the rotor to the outer tube is denoted as the tip clearance, which is nominally set to 1 mm in this work. The influence of the tip clearance on the turbine efficiency is given in Sec. IV. With the hub radius fixed at 19.6 mm for all turbines, the hub to tip ratio for the smallest tip clearance of 2 mm is 0.7. This will slightly reduce for turbines with a smaller tip clearance. The axial spacing between the guide vanes and the rotor, x_s, is nominally set to 1 mm. The influence of the axial spacing on the turbine performance is given in Sec. V.

III. SHROUDED ROTOR

For an unshrouded rotor as shown in Fig. 2, there are tip losses caused by the pressure difference between the suction and pressure side of the blade, leading to radial flow into the
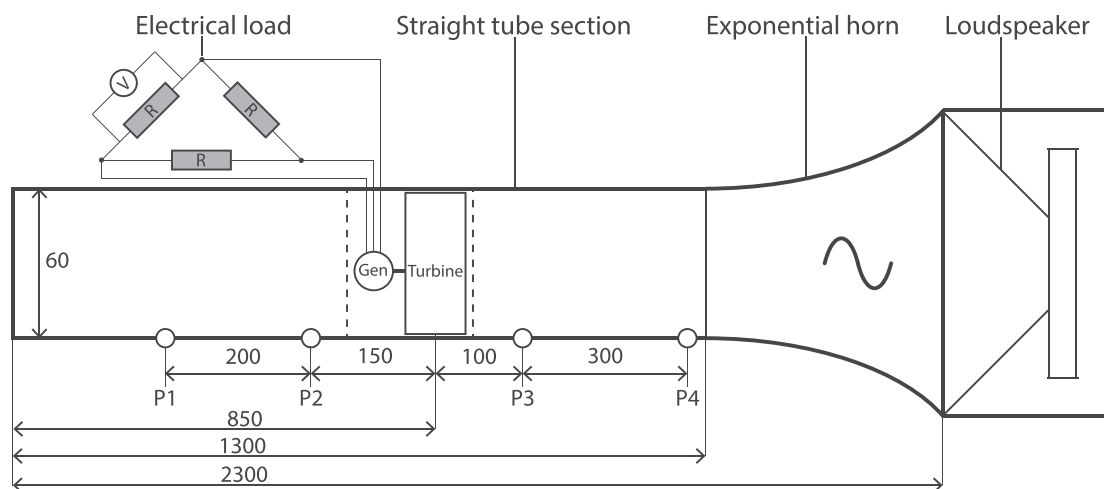

FIG. 1. Schematic of the experimental setup (not to scale). The pressure sensor locations (P1–P4) and tube dimensions are given in mm. A detailed schematic of the turbine section (depicted by the dashed lines) is given in Fig. 2. Note that this schematic is re-used from a previous publication (Ref. 8).
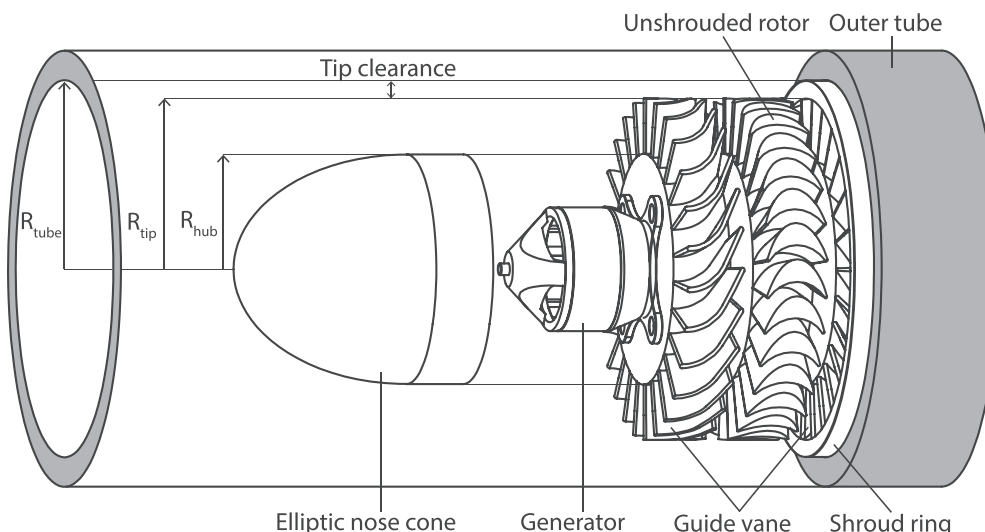
FIG. 2. Schematic of an axial bidirectional impulse turbine mounted in a tube section. The guide vanes are connected to the outer tube by a shroud ring (only depicted for the right guide vane). The generator is mounted on the left guide vane and connected to the rotor. During operation, the generator is enclosed by the nose cone, which also ensures the axial flow is redirected towards the guide vane blades. Besides the unshrouded rotor, also shrouded rotors are used in this work. Note that this schematic is re-used from a previous publication (Ref. 8).

gap between the outer tube and the tip of the blades.[10] This loss mechanism can be prevented by featuring a ring at the tip of the rotor blades, similar to the shroud ring shown for the guide vane in Fig. 2. For a shrouded rotor, the losses that remain are caused by the leakage flow around the rotor. Both loss mechanisms can be decreased by reducing the tip clearance, as will be investigated in Sec. IV. Here, the focus is on comparing an unshrouded rotor with a shrouded rotor for the same tip clearance of 1 mm. According to steady flow measurements by Yoon *et al.*, for this relatively large tip clearance compared to the tube radius of 30 mm, a shrouded rotor should perform significantly better.

The blades of the shrouded rotor are radially shorter by 1 mm, such that adding the 1 mm thick shroud ring provides the same tip clearance as for the unshrouded rotor. In Fig. 3,
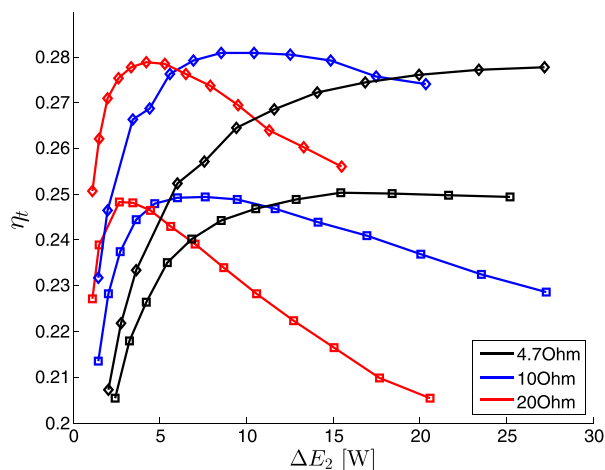

FIG. 3. (Color online) Turbine efficiency as a function of the acoustic power drop for an unshrouded and a shrouded rotor. The legend displays the resistance that is used for the electrical load. The unshrouded rotor is denoted by square (□) markers and the shrouded rotor by diamond (◇) markers. All results are for an acoustic frequency of 70 Hz.

the turbine efficiency is shown for both rotors as a function of the acoustic power drop and for varying turbine loads. It can be seen that the efficiency of the shrouded rotor is significantly higher than for the unshrouded rotor, reaching up to about 3% difference at the point of maximum efficiency. Furthermore, the maximum efficiency that can be reached for both cases is independent of the turbine load. Finally, just as shown for the unshrouded rotor in previous work,[8] it is found that the acoustic frequency has a negligible influence on the turbine efficiency for the shrouded rotor. It can therefore be said that the shrouded rotor outperforms the unshrouded rotor for all investigated operating conditions.

It is worth noting that the thickness of the shroud ring will also have an influence on the turbine performance, since it determines the blade height and thus the blade area of the rotor blades. Therefore, the influence of both a thinner and thicker shroud ring is investigated in Sec. IV. Furthermore, the current conclusion that a shrouded rotor is superior can only be made for the current tip clearance. In Sec. IV, the tip clearance will be varied for both unshrouded and shrouded rotors to check whether this conclusion is true in general.

IV. TIP CLEARANCE

Adding a shroud ring to the rotor has increased the maximum turbine efficiency to approximately 28%, but this is not yet in the same range as the 37% that Setoguchi *et al.* have measured in an OWC.[9] With the geometry of the blades being the same, the main difference in design is identified as the tip clearance. Setoguchi *et al.* have a 1 mm tip clearance for a 300 mm tube radius, resulting in a tip clearance ratio of $1/300 = 0.33\%$. This is more than ten times smaller than the tip clearance ratio of approximately 3.8% that has been used so far in this work. In this section the tip clearance is varied in an effort to increase the maximum

Michael A. G. Timmer and Theo H. van der Meer

turbine efficiency, and more generally to identify the influence of the tip clearance under thermoacoustic conditions. This is done for both shrouded and unshrouded turbines, since it has been shown that for steady flow turbomachinery an unshrouded turbine can become more efficient than a shrouded one for a small tip clearance.[10] Note that since the tube radius in the experimental setup is only 30 mm, and the 3D printed turbines have a tolerance of 0.2 mm, the smallest tip clearance ratio that can be achieved is around 1%.

Along with varying the tip clearance of the rotors, the thickness of the guide vane shroud ring is varied, such that the tip of the rotor blades is at the same radius as the tip of the guide vane blades (see R_{tip} and the guide vane shroud ring in Fig. 2). For the unshrouded rotor, measurements have also been done by keeping the same nominal guide vane while changing the rotor tip clearance. This can be used to identify the influence of the tip radius of the guide vane blades. The thickness of the rotor shroud ring has been kept at 1 mm, except for two rotors at 2% tip clearance ratio, where also a 0.5 and 1.5 mm shroud ring has been used to investigate the influence of the ring thickness. To make a concise comparison between all the different cases, only the maximum turbine efficiency for a 10 Ω load and a 70 Hz acoustic frequency is considered here. It can be seen from the Fig. 3 that this is a representative indicator, but the results for all measurements under varying operating conditions can also be found in the supplementary data publication.[11]

Figure 4 presents the maximum turbine efficiency as a function of the tip clearance ratio for all the turbines described in the previous paragraph. The most important thing to notice is that for the smallest tip clearance the turbine efficiency is more than 36%, thus reaching the same performance level as measured in OWCs,[9] even though the tip clearance ratio is still about three times larger here. For

the unshrouded rotor, the turbine efficiency for increasing tip clearance also decreases similarly as computed by Thakker and Dhanasekaran for a bidirectional impulse turbine oscillating flow.[14] This approximately linear relation between tip clearance and turbine efficiency, as well as the more parabolic relation for the shrouded rotor, is also found for steady flow measurements, albeit for significantly different turbine designs.[10] Furthermore, the shrouded rotor is also more efficient than the unshrouded rotor for all tip clearances in the examined range. However, when extrapolating the trend lines, it seems that the unshrouded rotor might become more efficient than the shrouded rotor for even smaller tip clearances. Such an effect has been experimentally measured by Yoon et al., who denote the crossing point as the break-even clearance. When examining the results for a 4.7 Ω turbine load, it is found that the unshrouded rotor is already more efficient than the shrouded rotor for the smallest tip clearance, with a break-even clearance ratio of 1.4%. At this point, the unshrouded rotor for 10 Ω still has a 0.6% lower turbine efficiency than the shrouded one, while for 20 Ω this goes up to 1.1%. This difference for a varying turbine load is caused by the acoustic power, and therewith the pressure drop and velocity, at which the maximum efficiency occurs (as can be seen in Fig. 3).

An additional result that can be seen in Fig. 4 is the dashed red line, which represent measurements for varying tip clearance of the unshrouded rotor while keeping the same set of nominal guide vanes (with $R_{tip} = 29$ mm). For a large tip clearance, it can be seen that this turbine setup is slightly more efficient than for a turbine where the guide vane blades vary with the tip of the rotor blade, as represented by the solid red line. Similarly, the inverse is true for the smallest tip clearances. This result is as expected, since more blade area at a large radius will generally increase the turbine performance. What is maybe more interesting about these results is the consistency of them, even though the maximum difference in efficiency of 0.7% is small. This attends to the accuracy at which these measurements can be performed.

The final result that can be seen in Fig. 4 is the influence of the thickness of the rotor shroud ring, which is varied at a tip clearance ratio of 2%. For a 1.5 mm shroud ring, the maximum turbine efficiency is 30.8%, which increases to 32.5% for a 1 mm ring and 34.3% for a 0.5 mm ring. This influence is way more significant than varying the blade height of the guide vanes, and shows that the maximum turbine efficiency for the shrouded rotors can be further improved by minimizing the shroud ring thickness. The latter will also shift the break-even clearance to smaller values, showing that for the current experimental setup it is best to use shrouded rotors. For systems with much larger dimensions, it is easier to produce a turbine with a smaller tip clearance ratio or relative shroud ring thickness. For such circumstances, the unshrouded rotors could perform better than the shrouded ones. Following the trend line from Fig. 4, which is also confirmed by Yoon et al. to continue
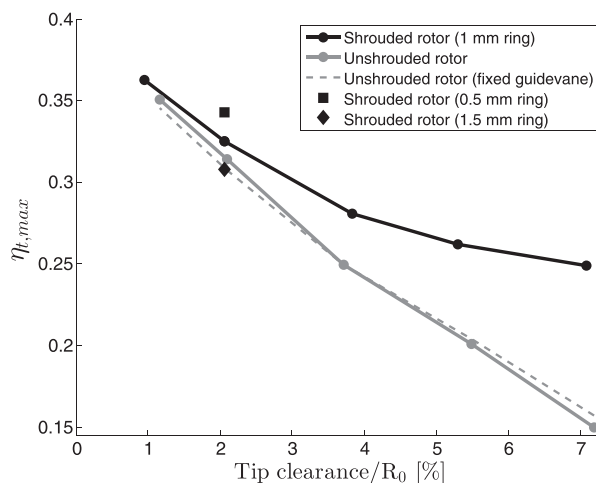

FIG. 4. Maximum turbine efficiency as a function of the tip clearance ratio, where $R_0 = 30$ mm and the radius of all rotors has been individually measured to determine the tip clearance. All maximum efficiencies are presented for a 10 Ω load resistance and 70 Hz acoustic frequency. The data for all 192 experiments with varying frequencies and loads can be found in the supplementary data publication (Ref. 11). Note that the two points around 3.8% tip clearance ratio correspond to the full performance curves given in Fig. 3.

for smaller tip clearance ratios,[10] the maximum turbine efficiency could reach up to 40%.

V. AXIAL SPACING

Where the tip clearance usually has a large affect on the performance of turbomachinery, as show in Sec. IV as well, the axial spacing between the guide vane and the rotor is generally less significant. Setoguchi *et al.* show that in OWCs with a frequency around 0.1 Hz, there is no influence of the axial spacing on the turbine efficiency.[9] Scaled to the dimensions of this work, they showed this for axial spacings from 1 to 8 mm. It is interesting to investigate whether this relative independence of axial spacing is also present in thermoacoustic conditions, since the frequency of oscillation is orders of magnitude higher, resulting in a much smaller displacement amplitude of the working fluid. So far all measurement have been done with an axial spacing of 1 mm. In this section, this is increased up to 6 mm, as well as decreased to 0.5 mm, where the latter is on the limit of what can be achieved in the experimental setup.

Figure 5 presents the maximum turbine efficiency as a function of seven different axial spacings. Results are presented for unshrouded rotors and shrouded rotors, both with two different tip clearance ratios. The first thing to notice is that there is a significant influence of the axial spacing on the turbine efficiency for all turbines. This effect is the biggest for the shrouded rotor with a large tip clearance ratio (5.3%). This can be explained by an interaction between the axial spacing and the tip clearance. As briefly described in Sec. III, the main tip clearance losses for a shrouded rotor are associated with a leakage flow around the rotor (as opposed to the unshrouded rotors where the dominant effect is leakage at the tip of the blades). When the spacing between the guide vane and rotor reduces, there is more resistance for the flow in the axial space to move radially outwards and subsequently flow around the shrouded rotor.

Since the rotor with the smaller tip clearance already has significantly less leakage flow, the influence of the axial spacing is not nearly as large here. Furthermore, it can be seen that for the smallest axial spacing of 0.5 mm, this shrouded rotor actually has a slightly smaller efficiency, which can also be seen for the unshrouded rotor with a small tip clearance. This effect has been measured in other work as well,[15] and can be explained by the increase in viscous losses due to the interaction between guide vane and rotor, which in this case outweighs the increase in performance by having a smaller spacing.

Another thing that can be seen in Fig. 5 is that the efficiency is higher for a smaller acoustic frequency as the axial spacing becomes larger. This might be an effect of the displacement amplitude of the working fluid, since for an equal axial velocity this is inversely proportional to the acoustic frequency. To look at this in more detail, the turbine efficiency as a function of the displacement amplitude is presented in Fig. 6 for a shrouded rotor with 1 mm and 6 mm spacing. For the 1 mm axial spacing measurements (in gray), it can be seen that the displacement amplitude at which the maximum turbine efficiency occurs is indeed higher for 50 Hz than for 70 Hz. Furthermore, reducing the resistance to the turbine load for 50 Hz further shifts this displacement amplitude higher, which is expected since the maximum turbine efficiency occurs at a larger acoustic power drop (as shown in Fig. 3). The important thing to notice is that, even though the varying operating conditions cause a different displacement amplitude at which the efficiency is at maximum, the actual value of the maximum is constant ($\approx$32%). So the displacement amplitude has no influence on the maximum turbine efficiency for 1 mm axial spacing in the investigated range. It can be seen in Fig. 6 that this is not true anymore for the measurements done with 6 mm spacing (in black). For the measurement with 20 Ω and 70 Hz, the turbine efficiency is now significantly lower than the cases where the maximum efficiency is at a larger displacement amplitude. Furthermore, when compared to the 1 mm axial spacing, the maximum turbine efficiency is
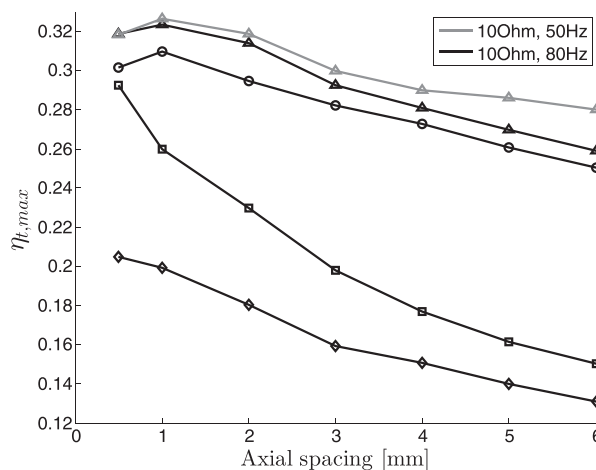
FIG. 5. Maximum turbine efficiency as a function of the axial spacing for two shrouded rotors and two unshrouded rotors. The shrouded rotors have a tip clearance ratio of 2.1% ($\triangle$ markers) and 5.3% ($\square$ markers). The unshrouded rotors have a tip clearance ratio of 2.1% ($\bigcirc$ markers) and 5.5% ($\diamond$ markers).
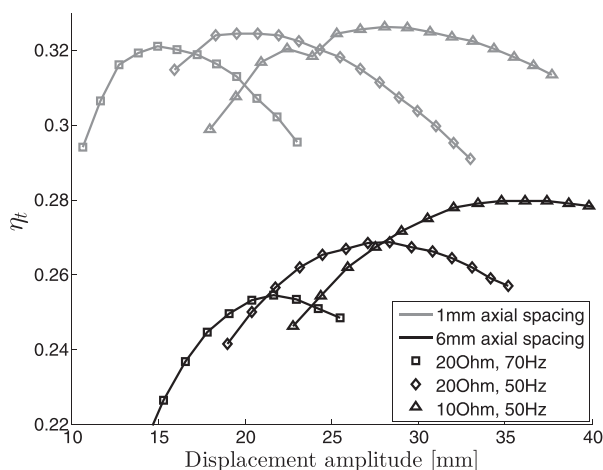
FIG. 6. Turbine efficiency as a function of the axial displacement amplitude for the shrouded rotor with a tip clearance ratio of 2.1%.

Michael A. G. Timmer and Theo H. van der Meer

reached at a larger displacement amplitude for all cases. Both of these effects show that for this relatively large spacing of 6 mm, there is a clear influence of the displacement amplitude, with a significant decrease in performance for smaller displacement amplitudes.

Now that it is shown that the displacement amplitude can (but does not always) have an effect on the turbine performance, it is interesting to quantify this behavior with respect to the axial spacing. For this purpose, Fig. 7 depicts the maximum turbine efficiency for a shrouded rotor as a function of the displacement amplitude divided by the axial spacing. A clear trend of dramatically decreasing turbine efficiency can be seen as the displacement amplitude of the working fluid approaches the length of the axial spacing. This is true for all generator loads and acoustic frequencies, as well as for the other shrouded rotor and two unshrouded rotors. For relatively large displacement amplitudes with respect to the axial spacing, the maximum turbine efficiency is approximately constant. This shows that for efficient operation, one needs to make sure that at the point of maximum turbine efficiency, the displacement amplitude is large enough with respect to the axial spacing. This has been shown to be true for all operating conditions at 1 mm spacing, while for 0.5 mm the efficiency even slightly decreased. Therefore, 1 mm axial spacing is concluded as optimal for the given turbine designs, and will be used in the remainder of this work.

VI. DESIGN STUDY

In Secs. III, IV, and V, the implementation of the turbine has been optimized under thermoacoustic conditions, such that the efficiency is in the same range as for OWCs. This has been done for a geometric design of the rotor and guide vanes that is shown to be optimal in OWCs using a design study.[9] In this section, a similar study is performed to investigate whether the shape of the guide vane and rotor blades is also optimal under thermoacoustic conditions.

The design of the guide vane and rotor blades that has been used so far is shown schematically in Fig. 8. The design is parameterized in such a way that all dimensions can be changed individually, while keeping the others constant. The values for the dimensions in Fig. 8 are for the reference geometry of the design study, for which the maximum turbine efficiency is measured to be approximately 37% for 10 Ω and 70 Hz. All design alterations in this section will be compared to the maximum efficiency of the reference design for the same operating conditions. Note that a tip clearance ratio of 1.3% and a shroud ring thickness of 0.7 mm is used. The guide vanes have a tip radius of 29 mm, such that the tip of the guide vane blades aligns with the tip of the rotor blades. If desired, a higher value of the turbine efficiency can be achieved by using guide vanes with a tip radius of 29.5 mm, a shroud ring thickness of 0.5 mm, and a smaller tip clearance ratio, as shown in Fig. 4. However, the aforementioned values are chosen since turbines with these dimensions can be more consistently 3D printed, which is the most important thing for the design study.

In Table I, the maximum turbine efficiency for several geometry variations is compared with the reference design. Since all measured efficiencies where found to be very similar, all measurements have been done twice and compared with the efficiency for the reference design that has been measured on the same day. The first two variations that are presented in Table I focus on the tip of the rotor blade, which are points that are specific for how the turbine is designed and produced in this work. In theory, the tip of the rotor blade should be smooth and thin, and follow the desired angle of the rotor, α_r. To provide a fully determined geometry with a circle on the pressure side and an ellipse on the suction side of the rotor, there is a need to slightly offset the local tip angles by $\Delta\alpha$ (see Fig. 8). Since this value is arbitrary, it was checked whether changing this to the minimum possible value of 6° and an equally larger value of 14° would affect the turbine efficiency. The results in Table I show that this is not the case, confirming that it is fair to define the effective tip angle of the rotor in this way. For the tip radius of the rotor blade, R_t, the larger value of 0.4 mm shows a slightly better efficiency. This could be insignificant, just as the value for 0.0 mm, since it is still in range of the measurement error. A possible explanation of why this bigger radius would be advantageous is because of the production technique. For a smaller radius the tip is more blunt, while a smooth radius will be more efficient, as was found by changing the tips of the guide vanes from blunt to smooth for some early stage prototypes (increasing the turbine efficiency by 4%).

With the topics specific to the implementation in this work treated, more general design variations can be investigated. In the remainder of Table I, the influence of the rotor length, thickness of the rotor blade, and the number of rotor blades is presented. First of all, the variations with changing number of blades are found to be insignificant. This is also
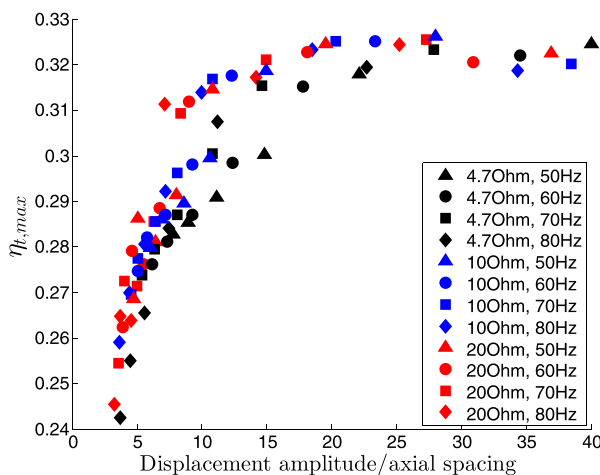

FIG. 7. (Color online) Maximum turbine efficiency as a function of the displacement amplitude divided by the axial spacing. Results are shown for all 84 experiments of the shrouded rotor with a tip clearance ratio of 2.1%. Similar results for the other shrouded rotor and two unshrouded rotors can be acquired from supplementary data publication (Ref. 11).
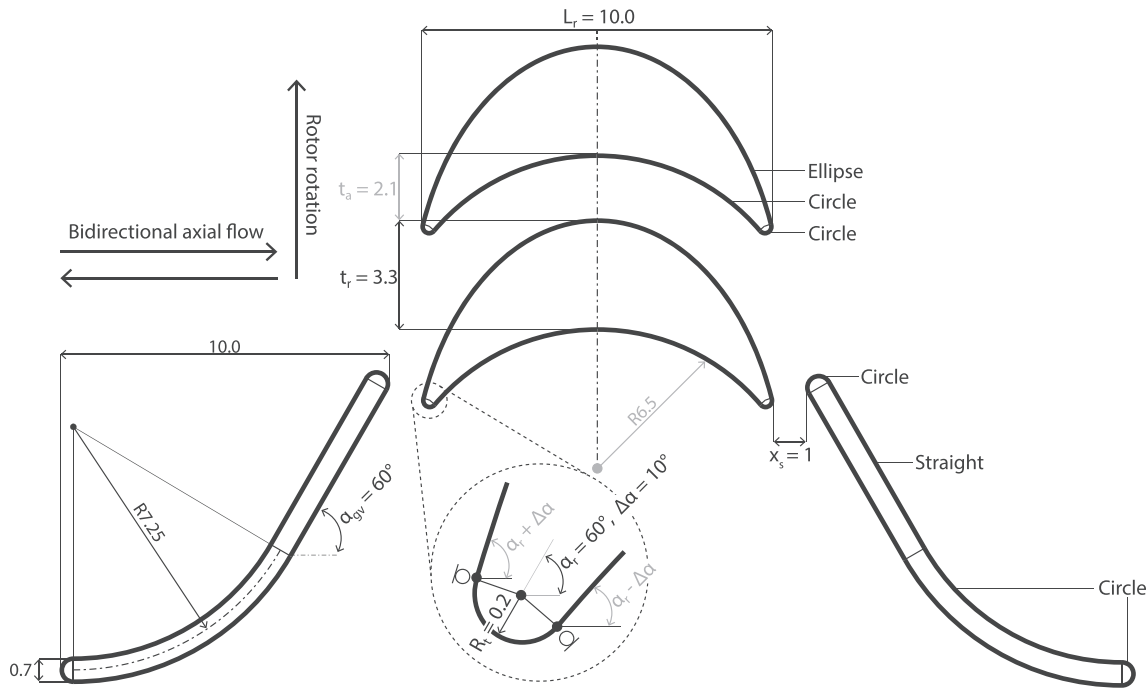
FIG. 8. Schematic of the bidirectional impulse turbine (to scale); adjusted from previous work (Ref. 8). The dimensions are given in mm unless stated otherwise, and provided at the mean turbine radius of 24.8 mm. All dimension are given for the reference turbine of the design study. The dimensions in black are exact (not rounded) and completely determine the geometry. The values in gray follow from the defined geometry and the number of blades. Note that in the zoomed section the symbol refers to lines being tangent at the corresponding points (♀) at the given angles.

the case for changing the chord length of the rotor blade, L_r, which is in contrast to what has been found in OWCs.[9,16] For the same relative variation in rotor chord length, an insignificant influence is found here, while a 1% and 3% reduction in turbine efficiency was found in OWCs. However, this was measured for turbines with self-pitching guide vanes, which makes a direct comparison invalid. The same holds true for the thickness of the rotor, which was again varied in relatively the same amount, but found to be of less influence. Nevertheless, there is a slight reduction in turbine efficiency measured for the smallest and largest rotor

TABLE I. For several geometry variations, the difference of the maximum turbine efficiency with respect to the reference geometry, $\Delta\eta_{t,max}$, is given. For each case, only a single design parameter is changed, with all other dimensions the same as given in Fig. 8.

	Reference design	Current design	$\Delta\eta_{t,max}$ [%]
$\Delta\alpha$	10°	6°	−0.1
		14°	−0.1
R_t	0.2 mm	0.4 mm	+0.7
		0.0 mm	+0.3
L_r	10.6 mm	8.6 mm	−0.2
		12.6 mm	+0.2
t_r	3.3 mm	3.7 mm	−0.7
		3.5 mm	+0.1
		2.9 mm	+0.7
		2.6 mm	−0.9
#blades	29	31	+0.1
		30	+0.1
		27	+0.2

thickness, while a t_r of 2.9 mm could be slightly better than the reference design. To summarize the results presented in Table I, it can be said that it is hard to draw the conclusion that specific design change are better or worse, since the measured differences are so small. This does, however, not mean that the results are not trustworthy, but simply that the presented design changes do not have a big influence on the turbine performance. In the remainder of this design study, it will be shown that similarly small design changes can have a more significant influence on the turbine efficiency.

Table II presents the maximum turbine efficiency for varying guide vane and rotor angles with respect to the reference case, where both angles are 60°. For fixed guide vanes and in oscillating flow, the 60° design was found to be significantly better than 50° or 70° in OWCs.[9,17] To narrow down on this range, turbines with matching guide vane and rotor blade angles of 55° and 65° are investigated here. Table II shows that the 55° turbine is 2.0% less efficient than the reference design, while the 65° turbine is 1.2% less efficient. This shows that when keeping the guide vane and rotor angle the same, a 60° turbine design is also superior for thermoacoustic conditions. However, what is also interesting from Table II is that a larger rotor angle for the 55° guide vane is more efficient, while a smaller rotor angle for the 65° guide vane is significantly less efficient. Note that such an influence was not reported for OWCs,[9,17] but this does show that the turbine with a 60° guide vane could be made more efficient. In the bottom part of Table II, this is indeed shown to be the case. Combining the 60° guide vane with a 65° rotor provides the highest turbine efficiency, while around 70° the efficiency equals that of the reference

2354   J. Acoust. Soc. Am. **147** (4), April 2020

Michael A. G. Timmer and Theo H. van der Meer

TABLE II. For varying guide vane and rotor angles, the difference of the maximum turbine efficiency with respect to the reference geometry, $\Delta\eta_{t,\max}$, is given. All other dimensions are the same as given in Fig. 8.

α_{gv}	α_r	$\Delta\eta_{t,\max}$ [%]
55°	55°	−2.0
	60°	−1.3
	65°	−1.1
65°	55°	−3.6
	60°	−2.1
	65°	−1.2
60°	55°	−1.3
	60°	(reference)
	65°	+1.2
	70°	+0.1
	73°	−0.1
	75°	−1.3

design again. Increasing the rotor angle further decreases the turbine efficiency, indicating that the optimum rotor angle for the 60° guide vane is indeed around 65°.

VII. CONCLUSIONS

The implementation of a bidirectional impulse turbine under thermoacoustic conditions is optimized to the extent that the maximum turbine efficiency is measured to be 38%. This is now in the same range as reported for similar turbine designs in OWCs. The largest increase in the turbine performance was found by minimizing the tip clearance, increasing the efficiency from 25% to 35% for an unshrouded rotor where the tip clearance ratio was reduced from 3.8% to 1.2%. For nearly all investigated tip clearance ratios, adding a shroud ring around the rotor blades is found to increase the turbine efficiency, especially when the tip clearance is relatively large. Only for a load resistance of 4.7 Ω at the smallest tip clearance, it is found that an unshrouded rotor performs better than a shrouded rotor. The break-even tip clearance ratio for this case is around 1.4%. However, reducing the thickness of the shroud ring from 1 to 0.5 mm is shown to further increase the turbine efficiency by 1.8%. For the current design, it can therefore be concluded that shrouded rotors will be the most efficient for the entire range that is investigated. Only when scaling to large enough sizes, where the relative tip clearance can be made small enough, the unshrouded rotors can become more efficient than the shrouded ones.

In contrast to OWCs, it is found that the axial spacing between the guide vanes and the rotor has a significant influence on the turbine efficiency, especially for a shrouded rotor with a relatively large tip clearance. For an increasing axial spacing, both the acoustic frequency as well as the turbine load start to have an effect on the efficiency. The deciding factor for this influence is identified as the displacement amplitude of the working fluid, where a significant decrease in turbine efficiency is measured when the displacement amplitude approaches the length of the axial spacing. For large enough displacement amplitudes with respect to the

spacing, the maximum turbine efficiency is found to be independent of this measure, therewith providing a range of operating conditions in which the turbine should be used for optimal performance.

For a shrouded rotor with a small tip clearance and spacing, a design study for the geometry of the guide vane and rotor blades is performed. The main purpose of the shape design study is to identify whether the optimal design for OWCs is also the best under thermoacoustic conditions. Since most design changes were found to only have a small effect on the turbine efficiency, it can be said that the reference design is in the right range, but it is hard to conclude that it is indeed optimal. For this purpose, future work could focus on more drastic design changes, or perform similar work for turbines at a larger scale, where the investigated design details will not be in the same order of magnitude as the accuracy of the production technique.

For the angle of the rotor and guide vanes, the measurements from the design study did show a significant influence on the turbine efficiency. From the results it can be concluded that a 60° turbine outperforms the ones with 55° and 65° angles. Furthermore, using a 60° guide vane along with a 65° rotor provides an additional increase in the turbine efficiency. When this design change is combined with further reducing the tip clearance, which should be possible for turbines at a larger scale, the results in this work show that a turbine efficiency of 40% should be achievable under thermoacoustic conditions.

[1]K. de Blok, "Novel 4-stage traveling wave thermoacoustic power generator," in *ASME 2010 3rd Jt. US-European Fluids Eng. Summer Meet. collocated with 8th Int. Conf. Nanochannels, Microchannels, Minichannels*, Montreal, Canada (2010), pp. 73–79.

[2]D. L. Gardner and C. Q. Howard, "Waste-heat-driven thermoacoustic engine and refrigerator," in *Acoust. 2009*, Adelaide, Australia (2009), pp. 1–4.

[3]R. Chen and S. L. Garrett, "A large solar/heat-driven thermoacoustic cooler," J. Acoust. Soc. Am. **108**(5), 2554–2554 (2000).

[4]Z. Wu, W. Dai, M. Man, and E. Luo, "A solar-powered traveling-wave thermoacoustic electricity generator," Sol. Energy **86**(9), 2376–2382 (2012).

[5]M. A. G. Timmer, K. De Blok, and T. H. Van Der Meer, "Review on the conversion of thermoacoustic power into electricity," J. Acoust. Soc. Am. **143**(2), 841–857 (2018).

[6]J. Callanan and M. Nouh, "Optimal thermoacoustic energy extraction via temporal phase control and traveling wave generation," Appl. Energy **241**, 599–612 (2019).

[7]A. F. Falcão and J. C. Henriques, "Oscillating-water-column wave energy converters and air turbines: A review," Renew. Energy **85**, 1391–1424 (2016).

[8]M. A. G. Timmer and T. H. Van Der Meer, "Characterization of bidirectional impulse turbines for thermoacoustic engines," J. Acoust. Soc. Am. **146**, 3524 (2019).

[9]T. Setoguchi, S. Santhakumar, H. Maeda, M. Takao, and K. Kaneko, "A review of impulse turbines for wave energy conversion," Renew. Energy **23**(2), 261–292 (2001).

J. Acoust. Soc. Am. **147** (4), April 2020

Michael A. G. Timmer and Theo H. van der Meer   2355

[10] S. Yoon, E. Curtis, J. Denton, and J. Longley, "The effect of clearance on shrouded and unshrouded turbines at two levels of reaction," J. Turbomach. **136**(2), 021013 (2013).

[11] M. A. G. Timmer, "Optimizing bidirectional impulse turbines for thermoacoustic engines," Dataset, 4TU. Centre for Research Data (2019). doi: 10.4121/uuid:09816a6f-cc1a-4f33-9499-11cf407b32b2.

[12] A. M. Fusco, W. C. Ward, and G. W. Swift, "Two-sensor power measurements in lossy ducts," J. Acoust. Soc. Am. **91**(4), 2229–2235 (1992).

[13] M. Suzuki, M. Takao, E. Satoh, S. Nagata, K. Toyota, and T. Setoguchi, "Performance prediction of OWC type small size wave power device with impulse turbine," J. Fluid Sci. Technol. **3**(3), 466–475 (2008).

[14] A. Thakker and T. Dhanasekaran, "Computed effects of tip clearance on performance of impulse turbine for wave energy conversion," Renew. Energy **29**(4), 529–547 (2004).

[15] K. Yamada, K.-i. Funazaki, M. Kikuchi, and H. Sato, "Influences of axial gap between blade rows on secondary flows and aerodynamic performance in a turbine stage," Proc. ASME Turbo Expo **7**, 11 (2009).

[16] H. Maeda, T. Setoguchi, K. Kaneko, T. W. Kim, and M. Inoue, "Effect of turbine geometry on the performance of impulse turbine with self-pitch-controlled guide vanes for wave power conversion," Int. J. Offshore Polar Eng. **5**(01), 378–382 (1995).

[17] H. Maeda, S. Santhakumar, T. Setoguchi, M. Takao, Y. Kinoue, and K. Kaneko, "Performance of an impulse turbine with fixed guide vanes for wave power conversion," Renew. Energy **17**(4), 533–547 (1999).

2356   J. Acoust. Soc. Am. **147** (4), April 2020

Michael A. G. Timmer and Theo H. van der Meer